Hole mobility improvement in Cu2O thin films prepared by the mist CVD method

AUTHOR(S):

Ikenoue, Takumi; Kawai, Toshikazu; Wakashima, Ryo; Miyake, Masao; Hirato, Tetsuji

Template for APEX (Jan. 2014)

Hole mobility improvement in Cu_2O thin films prepared by the mist CVD method.

Takumi Ikenoue*, Yoshikazu Kawai, Ryo Wakashima, Masao Miyake, and Tetsuji Hirato

Graduate School of Energy Science, Kyoto University, Kyoto, 606-8501, Japan

E-mail: ikenoue.takumi.4m@kyoto-u.ac.jp

A high-mobility Cu_2O thin film was fabricated using the mist chemical vapor deposition (CVD) method. This was achieved by suppressing the contamination from nitrogen impurities and optimum growth conditions to obtain single-phase Cu_2O without CuO. A 600 nm Cu_2O thin film was obtained using ethylenediaminetetraacetic acid as a complexing agent in dry-air growth atmosphere for 120 min. The resulting thin film had a resistivity of 2.8×10^{2} Ω·cm, carrier concentration of 1.2×10^{15} cm^{-3}, and hole mobility of 19.3 $cm^{2}\cdot V^{-1}\cdot s^{-1}$. This hole mobility improved by two or more orders of magnitude that of previous Cu_2O thin film obtained by mist CVD method.

Cuprous oxide (Cu_2O) has attracted considerable attention as a promising material for photovoltaic applications[1–7] owing to its high elemental abundance and nontoxicity. Cu_2O is a p-type oxide semiconductor with a direct bandgap of 2.0–2.1 eV[8] and high absorption coefficient of 10^4 cm^{-1} in the visible light region[9]. The current possible conversion efficiency of Cu_2O-based solar cells is greater than 8%[10,11], and further improvements are expected. For many of the highly efficient Cu_2O-based solar cells[10,12–14], Cu_2O sheets produced by thermal oxidation are used. The thermally oxidized Cu_2O sheets have excellent electrical characteristics, such as a high mobility, which require a high-temperature (>1000 °C) process. Furthermore, it is difficult to obtain a thin film suitable for solar cell applications. In addition, most other high-quality Cu_2O thin films[15–20] are obtained using a vacuum process and/or high-temperature process that is neither environmentally friendly nor low cost. In the use of non-vacuum and low temperature process, although there are a few reports of high quality Cu_2O thin films by the electrochemically deposition method[21,22], it is difficult to continuously produce solar cell laminate structure. Herein, we focus on mist chemical vapor deposition (CVD)[23–32] as a film-deposition method with a low environmental load and high productivity. The mist CVD technique allows the growth of high-quality films in atmosphere without vacuum equipment and can be easily applied for large substrates. However, the Cu_2O thin film obtained using the mist CVD method has a hole mobility of 0.2 $cm^2 \cdot V^{-1} \cdot s^{-1}$ [33], which is remarkably lower than that of Cu_2O (110 $cm^2 \cdot V^{-1} \cdot s^{-1}$) obtained by the thermal oxidation method. Similarly, the mobility of the Cu_2O thin film obtained by non-vacuum and low-temperature (solution) processes, such as atmospheric atomic layer deposition (AALD) and the molecular precursor method, is also low[7,14,20,33–38]. Representative studies on Cu_2O thin films are summarized in Table I. The improvement in the electrical characteristics of the Cu_2O thin film is indispensable for high-efficiency solar cell applications[39]. In particular, it is important to realize high mobility Cu_2O thin film using a method suitable for industrial application. Under atmospheric pressure (or a certain oxygen partial pressure condition), Cu_2O easily changes to CuO as the temperature rises. The mist CVD method is no exception, and the generation of CuO appears from approximately 400 °C. Therefore, Cu_2O thin films are grown in low-temperature conditions of less than 400 °C.

In this work, we report a dramatic improvement in the mobility of Cu_2O thin films by the

mist CVD method, i.e., an increase of two orders of magnitude, by controlling the complex forming material and film-growth atmosphere. A high-quality Cu_2O thin film that is comparable to one fabricated by the conventional high-temperature and/or vacuum process is realized by the mist CVD method. The latter is excellent in productivity at low environmental loads and leads to the realization of highly efficient oxide solar cells.

Prior to the growth of Cu_2O, soda-lime glass substrates were sequentially washed in acetone, methanol, and deionized water in an ultrasonic cleaner. The Cu_2O thin films were grown by the mist CVD method, described elsewhere in detail[25–27,30,32]. The growth conditions of Cu_2O are summarized in Table II. The precursor used for the Cu_2O thin-film growth was copper acetylacetonate, $Cu(acac)_2$, which was diluted in a solution of methanol and deionized water of concentration 0.020 mol/L. Etylenediamine (EDA) or ethylenediaminetetraacetic acid (EDTA), which is an additive for forming a complex together with copper ions, was added to the solution. In a previous study[33], EDA was used as a complex agent. In this case, two EDA molecules coordinate with one Cu atom to form a complex[40], as shown in Fig. 1 (a). In Fig 1 (a), the Cu atom coordinates only with the N atoms. The Cu_2O thin films grown using the EDA as a complex agent at a low temperature of 400 °C or less contained a considerable amount of N atoms as impurities, which was indicated by the shifting peak of the XRD patterns to a higher angle, and nitrogen was detected by energy dispersive X-ray spectrometry (EDX). It is assumed that these N impurities lead to a decrease in mobility, so EDTA as a complex agent was investigated to suppress the incorporation of N. When EDTA was used as a complexing agent, one EDTA molecule and one Cu atom form a complex as shown in Fig. 1 (b). One Cu atom is coordinated with two N and four O atoms, and the suppression of the incorporation of N atoms is expected. To sufficiently promote the thermal decomposition reaction and oxidation reaction, even at low temperatures, dry air (N_2 80%, O_2 20%) was investigated as the carrier and dilution gas as well as the growth atmosphere. Conventional growth conditions with N_2 alone were tested for comparison. Furthermore, the film formation time was prolonged with the expectation of improvement in the electrical characteristics owing to the increase in crystal grain size.

First, the phase of the obtained samples was confirmed by XRD. The XRD patterns of the samples obtained under representative conditions is shown in Fig. 2. Although Cu_2O growth

was confirmed regardless of the complex agent, growth atmosphere, and growth time, the obtained sample was a single-phase Cu_2O at a growth temperature of 375 °C or below, and a mixed phase of Cu_2O and CuO at a growth temperature of 400 °C or above under any growth conditions. Interestingly, each diffraction position of the Cu_2O thin films represented by Cu_2O (111), shown in Fig. 2 (b), approached the reference position by further using EDTA as the complex agent, dry air as the growth atmosphere, and 120 min as the growth time. In addition, nitrogen was detected below the measurement limit in the EDS measurement, also indicating that contamination of the nitrogen impurity was suppressed.

The optical properties of the samples were characterized by visible spectrometry. Figure 3 shows the transmittance spectra and Tauc plot of the Cu_2O thin film obtained using EDTA as a complexing agent and dry air as the growth atmosphere for 120 min. In the transmittance spectra, the marked decrease in the transmission rate at a wavelength shorter than 600 nm is clearly due to the absorption by Cu_2O. The bandgap of the Cu_2O films calculated from the Tauc $((\alpha h\nu)^2–h\nu)$ plot was 2.02 eV, and was almost constant irrespective of the film growth conditions. This bandgap value agrees well with that of Cu_2O[41]. It is noteworthy that the thin film in which CuO was observed by XRD analysis, has a smaller band gap value, i.e., 1.2–1.8 eV[42], which is suggestive of the CuO bandgap.

The electrical resistivity was determined by the four-terminal method, using the film thickness determined by the cross-sectional SEM image. Van-der-Pauw–Hall measurements were performed at room temperature to characterize the electrical properties of the Cu_2O thin films. Hall measurements could not be performed on the Cu_2O thin film obtained using EDA as a complexing agent because of the measurement limits. All of the samples for which the Hall measurement could be performed exhibited p-type conductivity. Figure 4 shows the growth temperature influence on the (a) resistivity, (b) carrier concentration, and (c) mobility, of the Cu_2O thin films obtained under each growth condition (complexing agent, atmosphere, and growth time). Using EDTA as the complexing agent, the resistivity was reduced by approximately one order of magnitude, compared with that using EDA as the complexing agent. From the measurement limit, it was inferred that the Cu_2O thin film obtained using EDA as the complexing agent had a low mobility of approximately 10^{-2} $cm^2 \cdot V^{-1} \cdot s^{-1}$ or less, and that the resistivity was lowered by a dramatic improvement in the hole mobility. By changing the growth atmosphere from N_2 to dry air, the resistivity further decreased. At a

growth temperature of 400 °C or below, the carrier concentration slightly decreased, mobility improved by approximately one order of magnitude, and resistivity decreased overall. This may be due to the promotion of the thermal decomposition reaction by O_2 in dry air, which reduces N impurities and contributes to a lower carrier concentration and mobility. However, at a growth temperature of 425 °C or above, the electrical characteristics were reversed, and the hole mobility of the Cu_2O grown in a dry air atmosphere dropped significantly. This is because the O_2 in dry air promotes not only the thermal decomposition reaction but also the oxidation of Cu_2O to CuO, such that the proportion of CuO in the film abruptly increased. Increasing the growth time further improved the hole mobility. At a growth time of 30 min, the film thickness was 150 nm, and the particle diameter of Cu_2O observed from the SEM image was approximately the same. Assuming that the growth time was 120 min, the film thickness was 600 nm and the particle diameter also increased to approximately 600 nm. This increase in grain size was thought to suppress the grain boundary scattering and improve the mobility.

Figure 5 shows the crystallite size of Cu_2O obtained under each growth condition. The relationship between the X-ray diffraction peak width and crystallite size is expressed by the following Scherrer equation:

$$\tau = \frac{K\lambda}{\beta \cos\theta}.$$

Here, $K = 1.15$ is the shape factor, $\lambda = 0.154$ nm is the X-ray wavelength, β is the full width at half maximum (rad) of the peak, θ is the Bragg angle (rad), and τ is the average size (nm) of the crystallite. From the XRD results, the diffraction peak of Cu_2O (111) was used to calculate the crystallite size. Figure 5 shows that the crystallite size of Cu_2O gradually increased when using the EDTA as the complexing agent and dry air as the growth atmosphere, with a 120 min growth time. Therefore, the increase in the crystallite size was correlated with the improvement in electrical characteristics. Figure 6 shows the influence of the crystallite size on the (a) resistivity and (b) mobility. The resistivity slightly decreased as the crystallite size increased. Similarly, the carrier concentration also slightly decreased as the crystallite size increased. However, the hole mobility abruptly increased as the crystallite size increased. The mobility was improved by approximately one order of magnitude by increasing the crystallite size by 5 nm. Hence, we conclude that the optimization of the growth conditions that increase the crystallite size is effective for

improving the hole mobility of Cu_2O. A Cu_2O thin film of resistivity 2.8×10^2 Ω·cm, carrier concentration 1.2×10^{15} cm^{-3}, and hole mobility 19.3 $cm^2\cdot V^{-1}\cdot s^{-1}$ was obtained using EDTA as the complexing agent, dry air as the growth atmosphere, and 120 min as the growth time at a growth temperature of 375 °C. This is one of the best hole mobility value attained in a Cu_2O thin film fabricated by a non-vacuum and low-temperature (solution) process, and this hole mobility improved by two or more orders of magnitude compared with that of previous Cu_2O thin film obtained by mist CVD method.

In conclusion, a high-mobility Cu_2O thin film was obtained using the mist CVD method. To grow a Cu_2O thin film with excellent electrical characteristics by the mist CVD method, the following two criteria must be met: (i) growth at 375 °C or below, in which a Cu_2O single phase is obtained instead of a mixed phase with CuO, and (ii) improvement of the crystallite size by suppressing N impurities and improving crystallinity. The Cu_2O thin film obtained using EDTA as the complexing agent and a dry-air growth atmosphere for 120 min of growth exhibited a hole mobility of 19.3 $cm^2\cdot V^{-1}\cdot s^{-1}$. We found that the improvement in the electrical characteristics, particularly the hole mobility, correlated with the improvement in the crystallite size. Combined with n-type oxide semiconductors such as ZnO and Ga_2O_3, which have already been realized with high quality by the mist CVD method, the development of highly efficient solar cell devices is expected.

Acknowledgments

This work was partially supported by the JSPS Grant-in-Aid for Young Scientists B (JP25870613) and Grant-in-Aid for Early-Career Scientists (JP18K13788).

References

1) L.C. Olsen, F.W. Addis, and W. Miller, Sol. Cells **7**, 247 (1982).

2) K. Fujimoto, T. Oku, and T. Akiyama, Appl. Phys. Express **6**, 086503 (2013).

3) C. Jayathilaka, V. Kapaklis, W. Siripala, and S. Jayanetti, Appl. Phys. Express **8**, 065503 (2015).

4) Y. Ievskaya, R.L.Z. Hoye, A. Sadhanala, K.P. Musselman, and J.L. MacManus-Driscoll, Sol. Energy Mater. Sol. Cells **135**, 43 (2015).

5) Y.S. Lee, D. Chua, R.E. Brandt, S.C. Siah, J.V. Li, J.P. Mailoa, S.W. Lee, R.G. Gordon, and T. Buonassisi, Adv. Mater. **26**, 4704 (2014).

6) S.W. Lee, Y.S. Lee, J. Heo, S.C. Siah, D. Chua, R.E. Brandt, S.B. Kim, J.P. Mailoa, T. Buonassisi, and R.G. Gordon, Adv. Energy Mater. **4**, 1301916 (2014).

7) K. Matsuzaki, K. Nomura, H. Yanagi, T. Kamiya, M. Hirano, and H. Hosono, Appl. Phys. Lett. **93**, 202107 (2008).

8) F.L. Weichman, Phys. Rev. **117**, 998 (1960).

9) C. Malerba, F. Biccari, C. Leonor Azanza Ricardo, M. D'Incau, P. Scardi, and A. Mittiga, Sol. Energy Mater. Sol. Cells **95**, 2848 (2011).

10) T. Minami, Y. Nishi, and T. Miyata, Appl. Phys. Express **9**, 052301 (2016).

11) T. Minami and T. Miyata, Oyobuturi **8**, 677 (2017).

12) T. Minami, Y. Nishi, and T. Miyata, Appl. Phys. Express **8**, 022301 (2015).

13) T. Minami, Y. Nishi, and T. Miyata, Appl. Phys. Express **6**, 044101 (2013).

14) T. Minami, Y. Nishi, T. Miyata, and J. Nomoto, Appl. Phys. Express **4**, 062301 (2011).

15) B.S. Li, K. Akimoto, and A. Shen, J. Cryst. Growth **311**, 1102 (2009).

16) Y.S. Lee, M.T. Winkler, S.C. Siah, R. Brandt, and T. Buonassisi, Appl. Phys. Lett. **98**, 192115 (2011).

17) Y. Guo, H. Lei, L. Xiong, B. Li, Z. Chen, J. Wen, G. Yang, G. Li, and G. Fang, J. Mater. Chem. A **5**, 11055 (2017).

18) S.H. Wee, P.S. Huang, J.K. Lee, and A. Goyal, Sci. Rep. **5**, 16272 (2015).

19) G. Kaur, K.L. Yadav, and A. Mitra, Appl. Phys. Lett. **107**, 053901 (2015).

20) Z. Wang, P.K. Nayak, J.A. Caraveo-Frescas, and H.N. Alshareef, Adv. Mater. **28**, 3831 (2016).

21) S.K. Baek, Y.H. Kwon, J.H. Shin, H.S. Lee, and H.K. Cho, Adv. Funct. Mater. **25**, 5214 (2015).

22) Y. Takiguchi, A. Orisaka, and S. Miyajima, J. Electrochem. Soc. **164**, D802 (2017).

23) H. Nishinaka, T. Kawaharamura, and S. Fujita, Jpn. J. Appl. Phys. **46**, 6811 (2007).

24) T. Kawaharamura, H. Nishinaka, and S. Fujita, Jpn. J. Appl. Phys. **47**, 4669 (2008).

25) D. Shinohara and S. Fujita, Jpn. J. Appl. Phys. **47**, 7311 (2008).

26) H. Nishinaka, Y. Kamada, N. Kameyama, and S. Fujita, Jpn. J. Appl. Phys. **48**, 121103 (2009).

27) H. Nishinaka, Y. Kamada, N. Kameyama, and S. Fujita, Phys. Status Solidi **247**, 1460 (2010).

28) T. Ikenoue, N. Kameyama, and S. Fujita, Phys. Status Solidi C **8**, 613 (2011).

29) J. Piao, S. Katori, T. Ikenoue, and S. Fujita, Phys. Status Solidi A **209**, 1298 (2012).

30) K. Akaiwa and S. Fujita, Jpn. J. Appl. Phys. **51**, 070203 (2012).

31) T. Ikenoue, H. Nishinaka, and S. Fujita, Thin Solid Films **520**, 1978 (2012).

32) N. Suzuki, K. Kaneko, and S. Fujita, J. Cryst. Growth **364**, 30 (2013).

33) T. Ikenoue, S. Sakamoto, and Y. Inui, Jpn. J. Appl. Phys. **53**, 05FF06 (2014).

34) G. Aggarwal, C. Das, S. Agarwal, S.K. Maurya, P.R. Nair, and K.R. Balasubramaniam, Phys. Status Solidi RRL **12**, 1700312 (2018).

35) K. Matsuzaki, K. Nomura, H. Yanagi, T. Kamiya, M. Hirano, and H. Hosono, Phys. Status Solidi A **206**, 2192 (2009).

36) V. Figueiredo, E. Elangovan, R. Barros, J. V Pinto, T. Busani, R. Martins, and E. Fortunato, J. Disp. Technol. **8**, 41 (2012).

37) D. Muñoz-Rojas, M. Jordan, C. Yeoh, A.T. Marin, A. Kursumovic, L.A. Dunlop, D.C. Iza, A. Chen, H. Wang, and J.L. MacManus Driscoll, AIP Adv. **2**, 042179 (2012).

38) H. Nagai, T. Suzuki, H. Hara, C. Mochizuki, I. Takano, T. Honda, and M. Sato, Mater. Chem. Phys. **137**, 252 (2012).

39) Y. Takiguchi and S. Miyajima, Jpn. J. Appl. Phys. **54**, 112303 (2015).

40) F.H. Allen, Acta Crystallogr. Sect. B Struct. Sci. **58**, 380 (2002).

41) M. Heinemann, B. Eifert, and C. Heiliger, Phys. Rev. B **87**, 115111 (2013).

42) A.Y. Oral, E. Menşur, M.H. Aslan, and E. Başaran, Mater. Chem. Phys. **83**, 140 (2004).

Figure Captions

Fig. 1. Complex formation of Cu using (a) EDA and (b) EDTA as complexing agents.

Fig. 2. (a) XRD patterns of Cu_2O thin films obtained under representative conditions. (b) Relative shift in Cu_2O (111) peak.

Fig. 3. (a) Transmittance spectra and (b) Tauc plot of Cu_2O thin film obtained using EDTA as a complexing agent.

Fig. 4. Growth temperature influence on (a) resistivity, (b) carrier concentration, and (c) hole mobility of the Cu_2O thin film obtained under each growth condition.

Fig. 5. Crystallite size for each growth condition calculated from the Cu_2O (111) diffraction peak.

Fig. 6. Crystallite size influence on (a) resistivity and (b) hole mobility.

Table I. A brief summary of the properties of representative Cu_2O thin films

Method		Substrate	T_{growth} [°C]	T_{anneal} [°C]	μ [$cm^2 V^{-1} s^{-1}$]	Ref
Vacuum	RF-magnetron sputtering	Glass	600	-	256	15)
	PLD	MgO (100)	700	-	90	33)
	RF-magnetron sputtering	Glass	RT	-	0.65	34)
			RT	200	18.47	
Atmospheric pressure	Thermal oxidation	-	1010	-	110	14)
	Electrochemically deposition	ITO	60	-	28.5	21)
	AALD	Glass	225	-	5.3	35)
	Molecular precursor	Glass	RT	450	4.8	36)
	Mist-CVD (previous)	Glass	350	-	0.2	31)
	Mist-CVD (this work)	Glass	375	-	19.3	

Table II. Growth condition of Cu_2O thin films.

Source, concentration	$Cu(acac)_2$, 0.050 mol/L
Complexing agent, concentration	EDA, 0.100 mol/L or EDTA, 0.050 mol/L
Solvent	H_2O:CH_3OH = 3:7
Carrier gas, flow rate	N_2 or Dry air, 3 L/min
Dilution gas, flow rate	N_2 or Dry air, 3 L/min
Growth temperature	350–450 °C
Growth time	30–120 min
Substrate, size	Soda lime glass, 25 mm × 25 mm

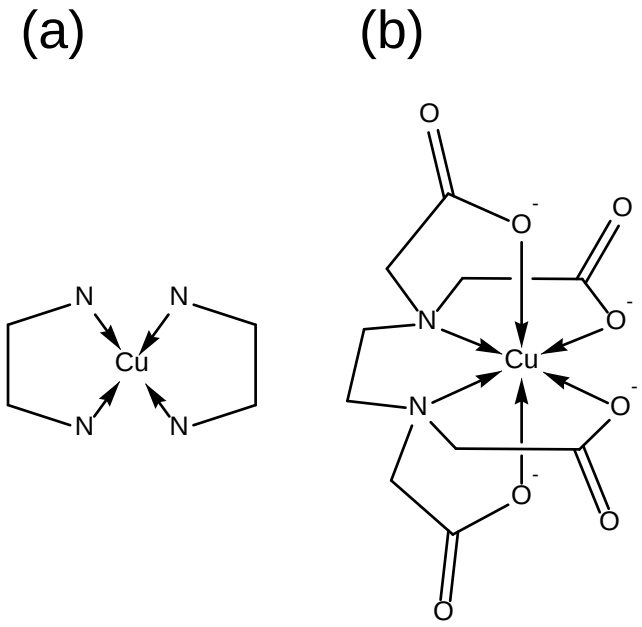

Fig.1.

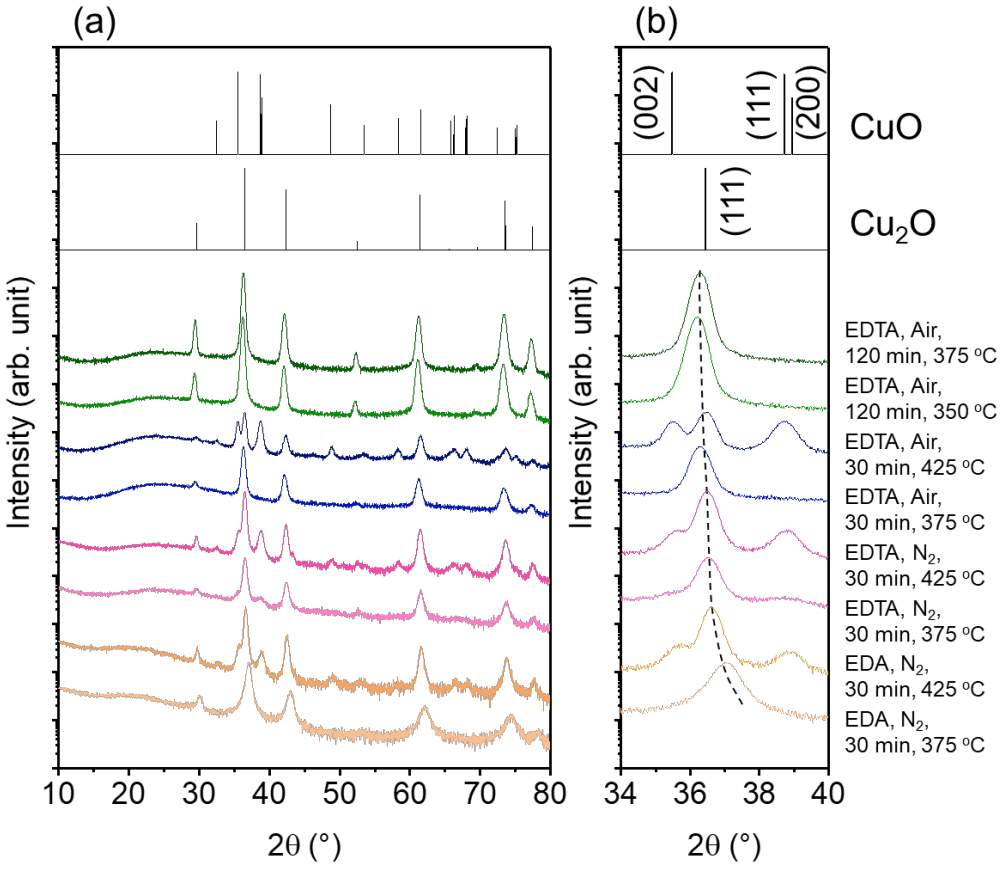

Fig. 2

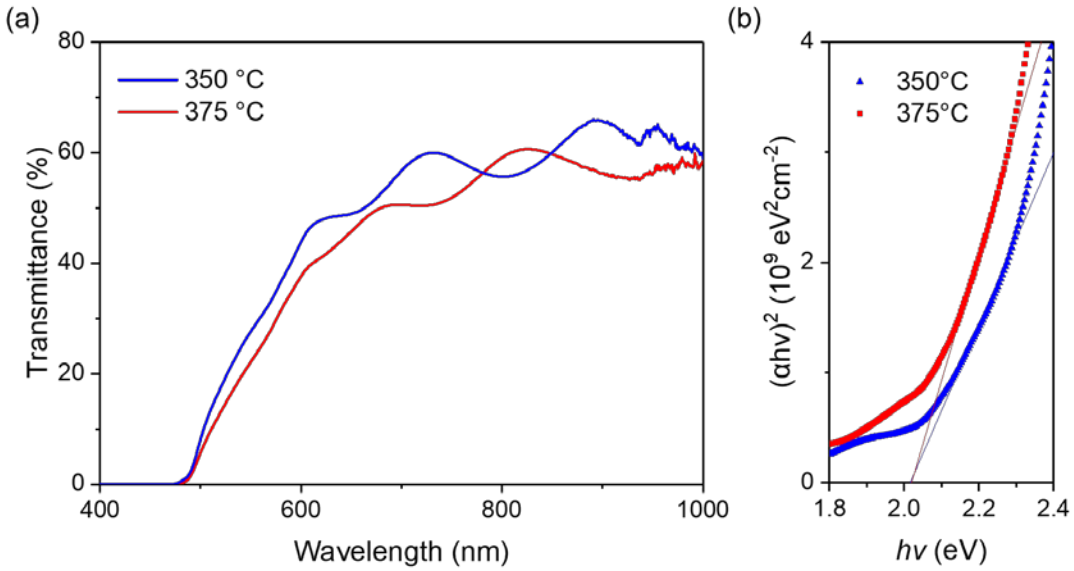

Fig. 3.

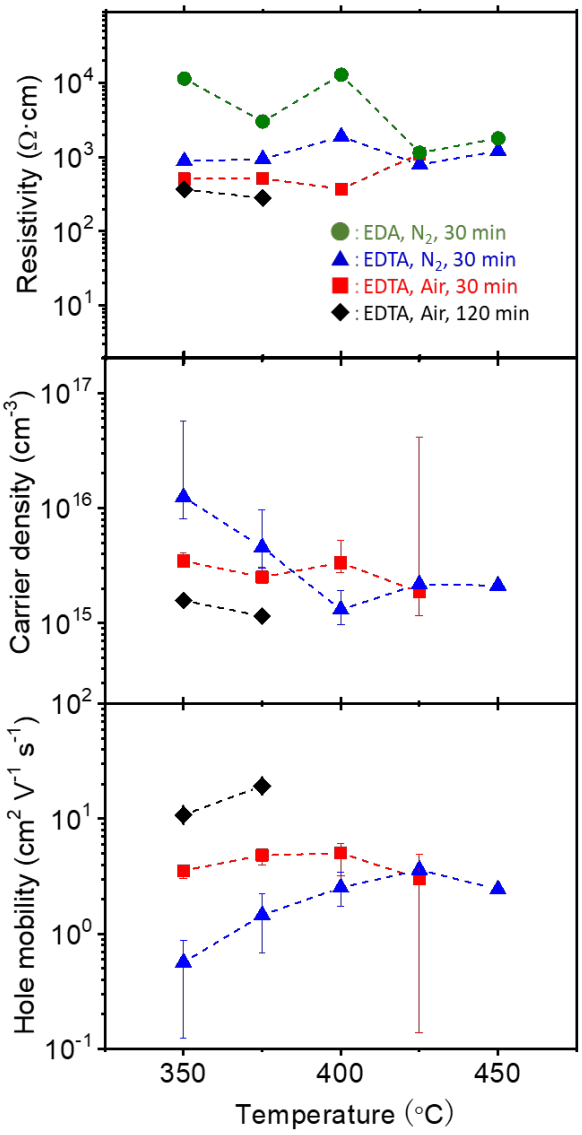

Fig. 4.

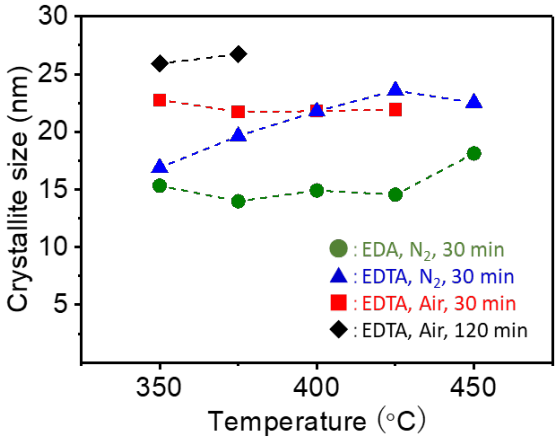

Fig. 5.

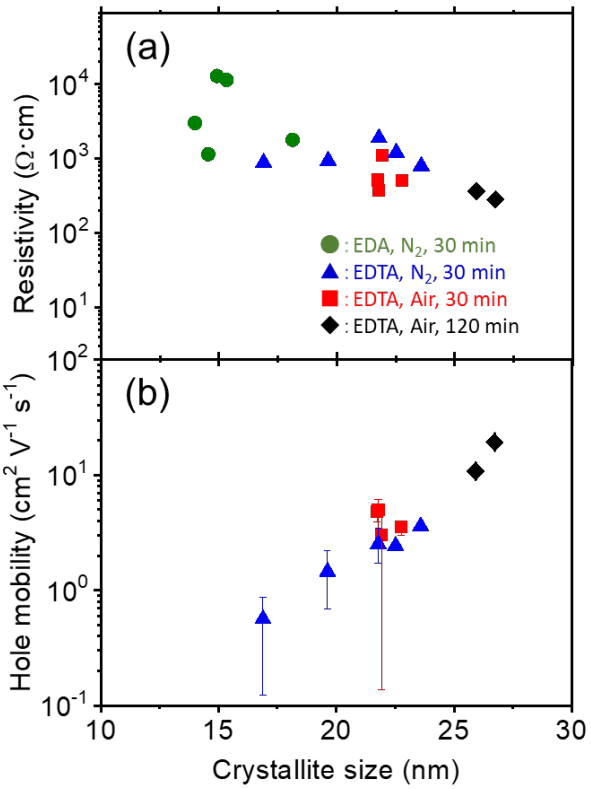

Fig. 6.